Experimental Electron Density Study of NaH_2PO_4 at 30 K

Mizuhiko Ichikawa,[a]* Torbjörn Gustafsson[b] and Ivar Olovsson[b]

[a]*Division of Physics, Graduate School of Science, Hokkaido University, 060-0810 Sapporo, Japan, and* [b]*Inorganic Chemistry, Ångström Laboratory, Uppsala University, Box 538, S-751 21 Uppsala, Sweden.*
E-mail: ichikawa@phys.sci.hokudai.ac.jp

Abstract

The deformation electron density of sodium dihydrogen phosphate, NaH_2PO_4, at 30 K has been studied as a reference for the electron-density characteristics of hydrogen-bonded ferroelectrics containing phosphate ions. Clear peaks of deformation electron density (0.3–0.6 e $Å^{-3}$) are seen in the middle of each P—O bond and electron deficiency (−0.2 to −0.4 e $Å^{-3}$) on the opposite side of each P—O bond peak. The peak height is higher and the peak shape is more distinct in P—O bonds than in P—O(H) bonds as a whole; the distribution of deformation density in the region of lone-pair electrons is more diffuse. The O—H···O bond deformation-density peaks of around 0.2 e $Å^{-3}$ appear in the middle of the O—H bond, followed by a deeper electron depletion of around −0.4 e $Å^{-3}$ on the H···O contract, just outside the H atom. The effective charges, defined as the integral of the deformation electron density, have the following values: around +0.2 for Na, +1.8 for P, −0.8 for O and +0.6 for H. The correlation of the deformation-density peaks and the depth of the negative peak of the H atom with the hydrogen-bond distance are discussed.

1. Introduction

Some inorganic phosphate compounds constitute an important group of materials exhibiting structural phase transitions. KH_2PO_4 (KDP) is the most typical hydrogen-bonded ferroelectric among them and an understanding of its phase-transition mechanism and the origin of the large isotope effect on the transition temperature T_c has been one of the central issues for more than five decades (Busch, 1987). The electric polarization is one of the fundamental physical quantities in ferroelectrics. However, comparison with the observed spontaneous polarization is often based on a formal point charge assigned to each atom, which seems unrealistic, especially in the case of a high valence atom such as phosphorus in an orthophosphate group. Therefore, even in the framework of the point-charge model, obtaining the effective charge based on the detailed electron-density distribution is necessary to obtain a deeper understanding of the origin of the macroscopic electric polarization from a microscopic point of view. There seems to be no published

deformation-density work on hydrogen-bonded ferroelectrics, as far as we are aware. This may be due to the following factors, which make accurate deformation-density studies rather difficult. First, the compounds often contain heavy elements. Second, in the ordered ferroelectric state with spontaneous polarization below T_c, obtaining a single-domain specimen is difficult since the crystal normally has multidomains. On the other hand, the electron density in the paraelectric phase above T_c is the average of two ferroelectric states with opposite polarity in time and space. The resultant higher symmetry imposed on the constituent moieties of the compound (*e.g.* fourfold rotoinversion in the PO_4 group in the case of KDP) may make it difficult to refine the deformation model and to deduce the deformation density in the ferroelectric state from that in the paraelectric one.

For the above reasons, as well as those listed below, we have chosen NaH_2PO_4 as a suitable substance for an accurate deformation-density study. Since NaH_2PO_4 has no ferroelectric transition, it is free from domain problems and may serve as a reference for the electron-density characteristics of hydrogen-bonded ferroelectrics containing XO_4 tetrahedral ions (X = P, As, S, Se). NaH_2PO_4 has the advantage that (i) it does not contain heavy elements, (ii) there are two independent PO_4 groups with no symmetry constraints and (iii) there are four independent, rather strong hydrogen bonds in an interesting range (2.50–2.65 Å; Catti & Ferraris, 1974), which allows us to study the correlation between deformation density and hydrogen-bond distance. Furthermore, neutron diffraction results are available (although only at room temperature; Choudhary *et al.*, 1981). The purpose of this study is to elucidate the basic characteristic features of the deformation electron density in the constituent atoms common to ferroelectrics and to estimate the net charge for each atom.

2. Experimental

Single crystals of NaH_2PO_4 were grown by evaporation of a saturated aqueous solution containing NaOH and excess H_3PO_4 compared with the stoichiometric ratio at around 353 K. A truncated pyramidal crystal with a (010)

basal plane was used; boundary planes $(1\bar{1}0)$, $(\bar{1}\bar{1}0)$, (010), $(0\bar{1}0)$, $(0\bar{1}1)$, $(00\bar{1})$; $V = 4.5 \times 10^{-3}$ mm³. Mo $K\alpha_1$ $(\lambda = 0.70930$ Å) was used for the determination of cell parameters.

The diffractometer was equipped with a 400 mm χ circle and a two-stage helium refrigerator (Samson *et al.*, 1980). The scan step width was $0.01°$ in ω with a minimum number of 70 steps plus $\alpha_1 - \alpha_2$ splitting. The measuring time varied from 0.3 to 3.0 s per step in the range $2 < 2\theta < 30°$ for $-4 \leq h \leq 4$, $-9 \leq k \leq 9$, $-5 \leq l \leq 5$, and in the range $30 < 2\theta < 105°$ for $-15 \leq h \leq 0$, $0 \leq k \leq 29$, $-16 \leq l \leq 16$ [$(\sin\theta/\lambda)_{max} = 1.1163$ Å⁻¹]. Six standard reflections, $\bar{1}12$, 004, 121, $\bar{2}30$, $\bar{3}0\bar{2}$ and $\bar{2}43$, were monitored over 680 h of total X-ray exposure time. The intensities and corresponding standard deviations were corrected for time variations by the method of McCandlish *et al.* (1975). The data set was corrected for background effects (Lehmann & Larsen, 1974) and Lorentz, polarization and absorption effects.

3. Refinements

The refinement started with the room-temperature structure reported by Catti & Ferraris (1974). The function minimized was $\Sigma w(F_o^2 - F_c^2)^2$ with $w = 1/\sigma^2(F^2)$, where $\sigma^2(F^2)$ was estimated from counting statistics and the scatter of the standard reflections. Final agreement indices *etc.* are given in Table 1.†

3.1. Extinction correction

A type I isotropic extinction parameter with Lorentzian distribution resulted in the best agreement between observed and calculated data (Becker & Coppens, 1974). In the final deformation refinement, 34 reflections had an extinction coefficient $y < 0.9$. The most severely affected reflection is 040 with $y = 0.66$, the next largest being $11\bar{2}$ with $y = 0.73$.

3.2. Deformation refinement

In the conventional spherical free-atom refinement all atoms except hydrogen were refined with anisotropic displacement parameters, the H atoms with an isotropic displacement parameter. The positional parameters for all atoms, including H atoms, were refined.

In the successive deformation refinements the deviation of electron density from spherical distribution was modelled by multipole functions according to the method

† Positional and anisotropic displacement parameters from the conventional refinement and deformation parameters, fractional atomic coordinates and displacement parameters of H atoms from neutron diffraction used for deformation refinement, hydrogen bonding distances, net charges and a list of structure factors for the deformation refinement have been deposited with the IUCr (Reference: AB0376). Copies may be obtained through The Managing Editor, International Union of Crystallography, 5 Abbey Square, Chester CH1 2HU, England.

Table 1. *Experimental details*

Crystal data	
Chemical formula	NaH₂PO₄
Chemical formula weight	119.98
Cell setting	Monoclinic
Space group	$P2_1/c$
a (Å)	6.8093 (8)
b (Å)	13.3936 (10)
c (Å)	7.2786 (10)
β (°)	92.827 (11)
V (Å³)	663.00 (13)
Z	8
D_x (Mg m⁻³)	2.404
Radiation type	Mo $K\alpha$
Wavelength (Å)	0.71073
No. of reflections for cell parameters	29
θ range (°)	25.00–31.60
μ (mm⁻¹)	0.793
Temperature (K)	30
Crystal form	Truncated pyramid
Crystal size (mm)	0.15 × 0.13 × 0.09
Crystal colour	Colourless
Data collection	
Diffractometer	Huber-Stoe–*ARACOR*
Data collection method	$\theta/2\theta$ scans
Absorption correction	Integration
T_{min}	0.8768
T_{max}	0.9129
No. of measured reflections	8836
No. of independent reflections	7760
No. of observed reflections	8836
Criterion for observed reflections	$I_{net} \geq -15\sigma(I_{net})$
R_{int}	0.014
θ_{max} (°)	52.50
Range of h, k, l	$-15 \rightarrow h \rightarrow 4$
	$-9 \rightarrow k \rightarrow 29$
	$-16 \rightarrow l \rightarrow 16$
No. of standard reflections	6
Frequency of standard reflections (min)	240
Intensity decay (%)	3.26
Refinement	
Refinement on	F^2
$R[F^2 > 2\sigma(F^2)]$	0.0207
$wR(F^2)$	0.0303
S	1.202
No. of reflections used in refinement	8836
No. of parameters used	547
H-atom treatment	H-atom parameters not refined
Weighting scheme	$w = 1/\sigma^2(F^2)$
$(\Delta/\sigma)_{max}$	0.100
$\Delta\rho_{max}$ (e Å⁻³)	0.28
$\Delta\rho_{min}$ (e Å⁻³)	−0.27
Extinction method	Isotropic type I, Lorentzian (Becker & Coppens, 1974)
Extinction coefficient	5.6×10^3
Source of atomic scattering factors	*International Tables for X-ray Crystallography* (Vol. IV)
Computer programs	
Data collection	*DIF4* (Stoe & Cie, 1992)
Cell refinement	*LATCON* (Lundgren, 1983)
Data reduction	Stoe–*DATR* (Lundgren, 1983)
Structure refinement	*DUPALS* (Lundgren, 1983)
Preparation of material for publication	*DISTAN* (Lundgren, 1983)

derived by Hirshfeld (1971) with the modifications of Harel & Hirshfeld (1975) and Hirshfeld (1977). Thus, the aspherical electron density $\delta\rho_a(r)$ at each atom site was expressed by an expansion of up to 35 terms (l) on the atomic centre with the general form

$$\delta\rho_a = \sum_l c_{a,l}\rho_{a,l}$$

with

$$\rho_{a,l}(r) = \rho_n(r_a, \theta_k) = N_n r^n \exp(-\gamma r^2)\cos^n \theta_k$$

centred on the atom site, where r and θ_k are polar coordinates in the kth of a chosen set of axes, n and k are integers $[n = 0, 1, 2, 3, 4; k = 1, \ldots, (n + 1)(n + 2)/2]$, l is a summation of k corresponding to up to $n = 4$ and N_n is a normalization factor. The parameters $c_{a,l}$ were refined. No symmetry constraints were imposed and a maximum of 35 deformation parameters up to $n = 4$ were refined for all atoms except hydrogen, for which four parameters up to $n = 1$ were used. The deformation refinement started with the final values from the conventional refinement. For the H atoms, the positional and displacement parameters obtained from neutron diffraction at room temperature (Choudhary *et al.*, 1981) were used for deriving low-temperature parameters because of the inaccuracy of the values from the X-ray refinement. We have assumed that the fractional coordinates do not change with temperature since NaH_2PO_4 has no transition; the anisotropic displacement parameters were estimated from those at room temperature assuming that the square of the displacement parameters is proportional to the absolute temperature.

A γ value of 4.0 was used for all atoms as a starting value. After convergence had been achieved, further refinements were performed to find the optimum γ values for each individual atom. The optimum γ value was searched by performing successive refinements with a shifted γ value for each atom, by using the weighted R value and the goodness-of-fit, and the sum of the square of the residuals as a measure of diagnosis. The optimum γ value was found to be 5.0 for Na, 4.0 for P, 3.5 for O and 4.0 for H. Residual electron density showed no special features around any atomic positions. The largest residual density was observed around the P2 atom with the maximum 0.28 and the minimum -0.27 e Å^{-3}.

4. Results and discussion

General features of the structure are described in earlier papers by Catti & Ferraris (1974) and Choudhary *et al.* (1981). A stereoscopic view of the structure is given in Fig. 1. Fractional atomic coordinates and equivalent isotropic displacement parameters are given in Table 2, selected bond lengths and angles in Table 3 and anisotropic displacement parameters in Table 4.

Table 2. *Fractional atomic coordinates and equivalent isotropic displacement parameters ($\mathring{A}^2$)*

$U_{eq} = (1/3)\Sigma_i\Sigma_j U^{ij} a_i^* a_j^* \mathbf{a}_i.\mathbf{a}_j.$

	x	y	z	U_{eq}
Na1	0.85875 (4)	0.40139 (2)	0.99759 (3)	0.00547 (6)
Na2	0.35350 (4)	0.39745 (2)	0.26659 (3)	0.00660 (7)
P1	0.32921 (2)	0.36906 (1)	0.85599 (2)	0.00311 (3)
P2	0.82484 (2)	0.36983 (1)	0.51328 (2)	0.00307 (3)
O1	0.24889 (4)	0.27573 (2)	0.76516 (4)	0.00556 (7)
O2	0.52194 (4)	0.34060 (2)	0.97813 (4)	0.00523 (7)
O3	0.19840 (4)	0.42762 (2)	0.97567 (4)	0.00488 (7)
O4	0.40596 (5)	0.44367 (2)	0.70630 (4)	0.00597 (7)
O5	0.92160 (4)	0.26881 (2)	0.57740 (4)	0.00569 (7)
O6	0.85200 (4)	0.44818 (2)	0.66203 (4)	0.00530 (7)
O7	0.92726 (5)	0.40282 (2)	0.33523 (4)	0.00547 (7)
O8	0.61026 (4)	0.34575 (2)	0.46694 (4)	0.00482 (7)

Table 3. *Selected geometric parameters ($\mathring{A}$, °)*

Na1—O2	2.4312 (5)	P2—O7	1.5653 (4)
Na1—O3^i	2.3525 (5)	P2—O8	1.5179 (4)
Na1—O3^{ii}	2.3327 (4)	O1—O2	2.5161 (5)
Na1—O5^{iii}	2.3860 (4)	O1—O3	2.5800 (4)
Na1—O6	2.5197 (5)	O1—O4	2.5362 (5)
Na1—O7^{iv}	2.4788 (5)	O2—O3	2.4916 (5)
Na2—O1^v	2.4262 (4)	O2—O4	2.5079 (5)
Na2—O2^{vi}	2.5576 (5)	O2—O8^{iii}	2.5696 (4)
Na2—O3^{vi}	2.3541 (5)	O3—O4	2.4822 (5)
Na2—O4^{vii}	2.6866 (4)	O4—O8	2.6324 (5)
Na2—O6^{vii}	2.5640 (4)	O5—O1^i	2.5578 (5)
Na2—O8	2.3262 (5)	O5—O6	2.5308 (4)
P1—O1	1.5044 (3)	O5—O7	2.5173 (5)
P1—O2	1.5947 (4)	O5—O8	2.4566 (5)
P1—O3	1.4979 (3)	O6—O7	2.5318 (5)
P1—O4	1.5858 (4)	O6—O8	2.5254 (5)
P2—O5	1.5659 (3)	O7—O6^{viii}	2.4978 (4)
P2—O6	1.5126 (3)	O7—O8	2.5232 (5)
O1—P1—O2	108.52 (2)	O5—P2—O6	110.57 (2)
O1—P1—O3	118.49 (2)	O5—P2—O7	107.01 (2)
O1—P1—O4	110.28 (2)	O5—P2—O8	105.60 (2)
O2—P1—O3	107.31 (2)	O6—P2—O7	110.67 (2)
O2—P1—O4	104.10 (2)	O6—P2—O8	112.88 (2)
O3—P1—O4	107.17 (2)	O7—P2—O8	109.83 (2)

(i) $\frac{1}{2} + x, y, z$; (ii) $1 - x, 1 - y, 2 - z$; (iii) $x, \frac{1}{2} - y, \frac{1}{2} + z$; (iv) $x, y, 1 + z$; (v) $x, \frac{1}{2} - y, z - \frac{1}{2}$; (vi) $x, y, z - 1$; (vii) $1 - x, 1 - y, 1 - z$; (viii) $2 - x, 1 - y, 1 - z$.

4.1. Deformation electron densities

4.1.1. *Sodium ion.* The appearance of the deformation densities around the two different Na atoms is similar. Viewing deformation densities in the planes perpendicular to the b axis (Fig. 2), both Na atoms are seen to have a deep cavity of electron deficiency at the centre. These two cavities are elongated along [101] and accompany two positive side peaks with 0.10–0.15 e Å^{-3}, which are also elongated in the same direction and approximately related by a pseudo-twofold axis parallel to the b axis through two atoms. These electron deficiencies point to two short contacts among the coordinated O atoms, which are approximately perpendicular to the ac plane for the Na1 atom and in

Table 4. *Anisotropic displacement parameters ($Å^2$) with standard deviations in parentheses*

The form of the displacement factor is $\exp(-2\pi^2 \Sigma_i \Sigma_j U^{ij} h_i h_j a_i^* a_j^*)$.

|	U^{11}	U^{22}	U^{33}	U^{12}	U^{13}	U^{23}
Na1	0.00492 (7)	0.00501 (6)	0.00646 (7)	−0.00024 (5)	−0.00002 (5)	0.00017 (5)
Na2	0.00734 (8)	0.00675 (7)	0.00556 (7)	0.00090 (6)	−0.00130 (6)	0.00004 (5)
P1	0.00284 (4)	0.00303 (4)	0.00344 (4)	0.00019 (2)	−0.00012 (2)	−0.00017 (3)
P2	0.00306 (4)	0.00287 (4)	0.00325 (4)	−0.00037 (2)	−0.00026 (2)	−0.00008 (3)
O1	0.00549 (8)	0.00449 (7)	0.00652 (8)	−0.00018 (6)	−0.00147 (6)	−0.00151 (6)
O2	0.00419 (8)	0.00447 (8)	0.00684 (8)	0.00076 (6)	−0.00169 (6)	0.00012 (6)
O3	0.00435 (8)	0.00522 (7)	0.00514 (8)	0.00107 (6)	0.00078 (6)	−0.00077 (6)
O4	0.00677 (8)	0.00552 (8)	0.00579 (8)	0.00081 (7)	0.00207 (6)	0.00141 (6)
O5	0.00517 (8)	0.00406 (7)	0.00761 (8)	0.00038 (6)	−0.00185 (6)	0.00098 (6)
O6	0.00621 (8)	0.00515 (7)	0.00455 (7)	−0.00140 (7)	0.00024 (6)	−0.00137 (6)
O7	0.00694 (8)	0.00512 (8)	0.00446 (8)	−0.00167 (7)	0.00148 (6)	−0.00015 (6)
O8	0.00330 (7)	0.00510 (7)	0.00598 (8)	−0.00067 (6)	−0.00071 (6)	−0.00011 (6)
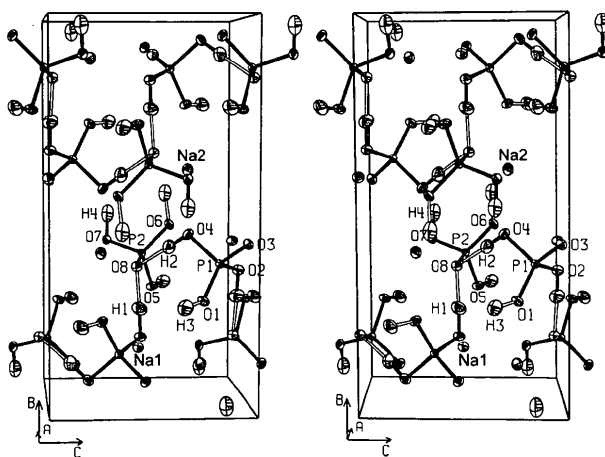
Fig. 1. A stereoscopic view (*ORTEP*II; Johnson, 1976) of the structure of NaH₂PO₄ at 30 K with displacement ellipsoids drawn at 90% probability. Covalent bonds are filled and hydrogen bonds open.
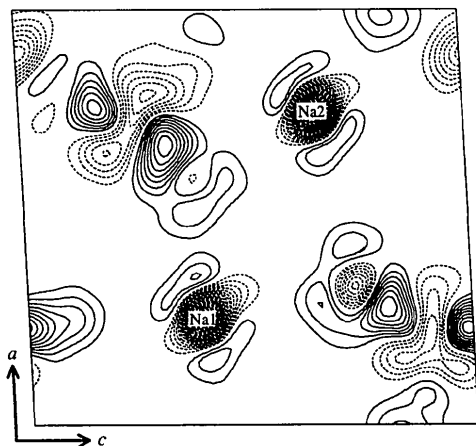

Fig. 2. The deformation electron density at $y = 0.4$. Contour intervals at 0.05 e $Å^{-3}$, positive contours are represented by full lines, negative contours dashed and zero levels are omitted.

the *ac* plane for the Na2 atom. This may indicate an anisotropy of the charge distribution of the Na atom which is located in a distorted coordination octahedron of O atoms.

4.1.2. Phosphate ion. The deformation densities in the O—P—O planes are given in Fig. 3. Peaks ranging from 0.3 to 0.6 e $Å^{-3}$ can be seen in the middle of each P—O bond. At the same time there is an electron deficiency (−0.2 to −0.4 e $Å^{-3}$) on the opposite side of phosphorus, which indicates that some charge is transferred into the P—O bond. On the whole, the peak height is higher and the peak shape clearer in the P—O bonds than in the P—O(H) bonds, as expected from the double-bond and
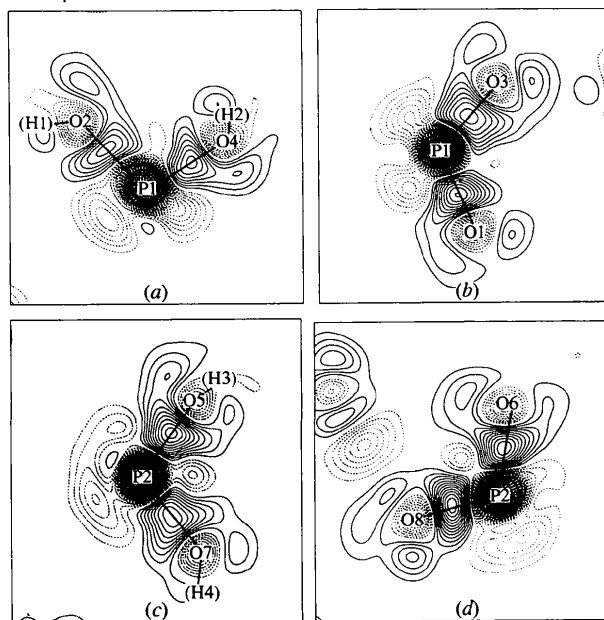

Fig. 3. Deformation electron density in the PO₄ ions: (*a*) O2—P1—O4 plane; (*b*) O1—P1—O3 plane; (*c*) O5—P2—O7 plane; (*d*) O6—P2—O8 plane. H atoms deviating from the planes are labelled in parentheses. Contour intervals *etc.* as given for Fig. 2.

single-bond characters, respectively [cf. Figs. 3(a) and (c) with Figs. 3(b) and (d)]. The deformation density in the region of the lone pairs is rather continuously distributed. For five O atoms the electron density in the lone-pair region showed distinct peaks and for three other O atoms it was more diffuse. The height of these peaks was 0.25 e Å^{-3} or less.

Earlier deformation-density work on phosphate-containing compounds includes KTiOPO$_4$, KTP (Hansen et al., 1991; Larsen, 1995) and H$_3$PO$_4$ (Moss et al., 1995; Souhassou et al., 1995). The overall features in our deformation-density maps around the PO$_4$ groups are similar to the dynamic and static deformation-density maps in these earlier studies.

4.1.3. *Hydrogen bonds.* The deformation-density features of the hydrogen bonds (Fig. 4) are those normally observed: clear deformation-density peaks of around 0.2 e Å^{-3} between oxygen and hydrogen followed by a deeper electron depletion of around −0.4 e Å^{-3}.

4.2. Net charge

In the Hirshfeld multipole refinement program, the net charge is obtained by integration over the atomic deformation density (Hirshfeld, 1977)

$$q = - \int \delta \rho_a(r) \mathrm{d}v.$$

During the process of refinements it was noticed that the net charges of some atoms depend considerably on their γ values (~30% in O, ~30% in H, ~10% in P on changing γ by 1.0 around the optimum value). Furthermore, it was recognized that the γ value of the O atom considerably affects the net charge of the atom covalently bonded to it (~35% in P and ~30% in H for a change of 1.0 around the optimum value 3.5). This demonstrates the difficulty of partitioning the electron charges between covalently bonded atoms. On the other hand, the net charges are rather close for the same elements, i.e. the two non-equivalent Na and P atoms, the eight O and four H atoms, respectively. The net charges in the NaH$_2$PO$_4$ crystal are much closer to the neutral values than to the formal charges. The net charges determined as described above are around +0.2 for Na, +1.8 for P, −0.8 for O and +0.6 for H.

It may not be fully justified to compare the values of the net charges using the different methods. However, in both the case of KTiOPO$_4$, KTP (Hansen et al., 1991), and NaH$_2$PO$_4$, the net charges of the P and O atoms are far from the formal charges and are closer to neutral, as is commonly observed. Furthermore, the net charge of the Na atoms of NaH$_2$PO$_4$ are in the range 0.1–0.5, as observed in earlier studies of compounds containing sodium ions (Bats et al., 1977).
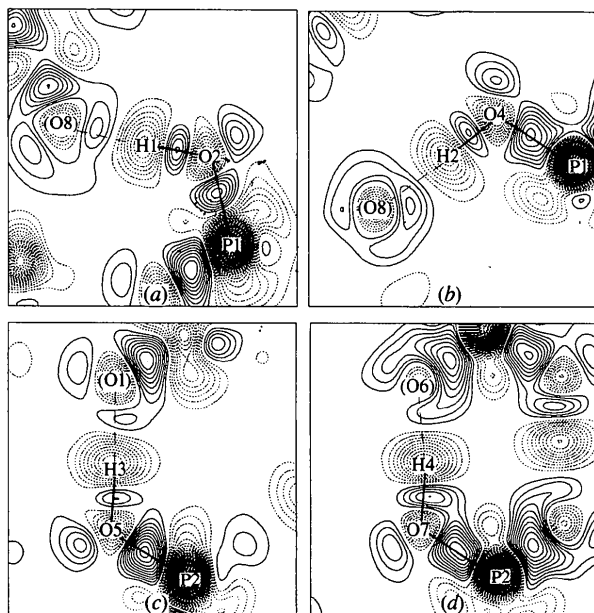

Fig. 4. The deformation electron density of the hydrogen bonds: (a) P1—O2—H1 plane; (b) P1—O4—H2 plane; (c) P2—O5—H3 plane; (d) P2—O7—H4 plane. Bonds to the O atoms deviating from the planes are drawn as dashed lines, these atoms are labelled in parentheses. Contour intervals etc. as given for Fig. 2.
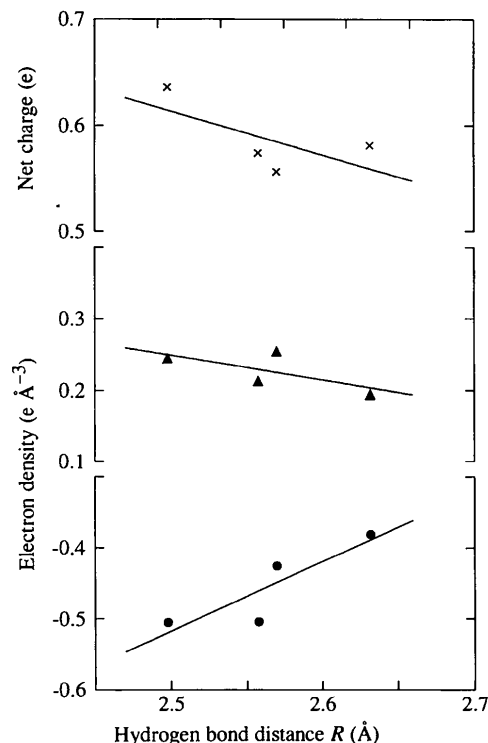

Fig. 5. Correlation between the hydrogen-bond distance and the net charge of the H atom (upper), the peak height (middle) and the depth of the negative peak at the proton site (lower). The least-squares lines are given only as a guide.

4.3. Possible correlations with hydrogen-bond parameters

The apparent correlations of net charge, deformation-density peaks of the O—H bond and depth of the negative peak at the hydrogen site with the hydrogen-bond distance are noteworthy (Fig. 5; see also Fig. 4), although it may be premature to draw a definite conclusion. With increasing hydrogen-bond distance, the peak height of the deformation density of the O—H bond decreases and the depth of deficiency in the electron density decreases. This may be explained by a decreased superposition with the positive peak on the acceptor O atom as the hydrogen-bond distance increases (cf. Olovsson et al., 1993). Similarly, the net charge of the H atoms appears to decrease with increasing the hydrogen-bond distance.

References

Bats, J. W., Coppens, P. & Kvick, Å. (1977). Acta Cryst. B33, 1534–1542.

Becker, P. J. & Coppens, P. (1974). Acta Cryst. A30, 129–153.

Busch, G. (1987). Editor. Ferroelectrics, Vol. 71. Special Issue on KH$_2$PO$_4$-Type Ferro- and Antiferroelectrics.

Catti, M. & Ferraris, G. (1974). Acta Cryst. B30, 1–6.

Choudhary, R. N. P., Nelmes, R. J. & Rouse, K. D. (1981). Chem. Phys. Lett. 78, 102–105.

Hansen, N. K., Protas, J. & Marnier, G. (1991). Acta Cryst. B47, 660–672.

Harel, M. & Hirshfeld, F. L. (1975). Acta Cryst. B31, 162–172.

Hirshfeld, F. L. (1971). Acta Cryst. B27, 769–781.

Hirshfeld, F. L. (1977). Isr. J. Chem. 16, 226–229.

Johnson, C. K. (1976). ORTEPII. Report ORNL-5138. Oak Ridge National Laboratory, Tennessee, USA.

Larsen, F. K. (1995). Acta Cryst. B51, 468–482.

Lehmann, M. S. & Larsen, F. K. (1974). Acta Cryst. A30, 580–584.

Lundgren, J.-O. (1983). Crystallographic Computing Programs. Report UUIC-B13-4-05. Institute of Chemistry, University of Uppsala, Sweden.

McCandlish, L. E., Stout, G. H. & Andrews, L. C. (1975). Acta Cryst. A31, 245–249.

Moss, G. R., Souhassou, M., Blessing, R. H., Espinosa, E. & Lecomte, C. (1995). Acta Cryst. B51, 650–660.

Olovsson, I., Ptasiewicz-Bak, H. & McIntyre, G. J. (1993). Z. Naturforsch. 48, 3–11.

Samson, S., Goldish, E. & Dick, C. J. (1980). J. Appl. Cryst. 13, 425–432.

Souhassou, M., Espinosa, E., Lecomte, C. & Blessing, R. H. (1995). Acta Cryst. B51, 661–668.

Stoe & Cie (1992). DIF4. Diffractometer Control Program. Stoe & Cie, Darmstadt, Germany.